

AperTO - Archivio Istituzionale Open Access dell'Università di Torino

Evaluation of PVA biodegradable electric conductive membranes for nerve regeneration in axonotmesis injuries: the rat sciatic nerve animal model

This is the author's manuscript

Original Citation:

Availability:

This version is available <http://hdl.handle.net/2318/1647231> since 2017-08-31T15:33:05Z

Published version:

DOI:10.1002/jbm.a.35998

Terms of use:

Open Access

Anyone can freely access the full text of works made available as "Open Access". Works made available under a Creative Commons license can be used according to the terms and conditions of said license. Use of all other works requires consent of the right holder (author or publisher) if not exempted from copyright protection by the applicable law.

(Article begins on next page)

This is the author's final version of the contribution published as:

Ribeiro, Jorge; Caseiro, Ana Rita; Pereira, Tiago; Armada-da-Silva, Paulo Alexandre; Pires, Isabel; Prada, Justina; Amorim, Irina; Leal Reis, Inês; Amado, Sandra; Santos, José Domingos; Bompasso, Simone; Raimondo, Stefania; Varejão, Artur Severo Proença; Geuna, Stefano; Luís, Ana Lúcia; Maurício, Ana Colette. Evaluation of PVA biodegradable electric conductive membranes for nerve regeneration in axonotmesis injuries: the rat sciatic nerve animal model. *JOURNAL OF BIOMEDICAL MATERIALS RESEARCH. PART A*. 105 (5) pp: 1267-1280.
DOI: 10.1002/jbm.a.35998

The publisher's version is available at:

<http://onlinelibrary.wiley.com/doi/10.1002/jbm.a.35998/fullpdf>

When citing, please refer to the published version.

Link to this full text:

<http://hdl.handle.net/>

Evaluation of PVA biodegradable electric conductive membranes for nerve regeneration in axotomy injuries: the rat sciatic nerve animal model

Jorge Ribeiro,^{1,2,3*} Ana Rita Caseiro,^{1,2,4*} Tiago Pereira,^{1,2} Paulo Alexandre Armada-da-Silva,^{5,6} Isabel Pires,^{7,8} Justina Prada,^{7,8} Irina Amorim,^{9,10,11} Inês Leal Reis,^{1,2} Sandra Amado,^{12,13} Jose Domingos Santos,⁴ Simone Bompasso,^{14,15} Stefania Raimondo,^{14,15} Artur Severo Proença Varejão,^{7,8} Stefano Geuna,^{14,15} Ana Lucia Luis,^{1,2,3} Ana Colette Mauricio^{1,2}

¹Departamento de Clinicas Veterinarias, Instituto de Ciencias^ Biomedicas de Abel Salazar (ICBAS), Universidade do Porto (UP), Rua de Jorge Viterbo Ferreira, n 228, Porto 4050-313, Portugal

²Sub-inidade de Cirurgia Experimental e Medicina Regenerativa, Centro de Estudos de Ciencia^ Animal (CECA), Instituto de Ciencias,^ Tecnologias e Agroambiente da Universidade do Porto (ICETA), Rua D. Manuel II, Apartado 55142, Porto 4051-401, Portugal

³UPVET, Instituto de Ciencias^ Biomedicas de Abel Salazar (ICBAS), Universidade do Porto (UP), Rua de Jorge Viterbo Ferreira, n 228, Porto 4050-313, Portugal

⁴CEMUC, Departamento de Engenharia Metalurgica e Materiais, Faculdade de Engenharia, Universidade do Porto, Rua Dr. Roberto Frias, Porto 4200-465, Portugal

⁵Faculdade de Motricidade Humana (FMH), Universidade de Lisboa (ULisboa), Estrada da Costa, 1499-002, Dafundo, Cruz Quebrada, Portugal

⁶CIPER-FMH: Centro Interdisciplinar de Estudo de Performance Humana, Faculdade de Motricidade Humana (FMH), Universidade de Lisboa (ULisboa), Estrada da Costa, 1499-002, Cruz Quebrada – Dafundo, Portugal

⁷Departamento de Ciencias^ Veterinarias, Universidade de Tras-os-Montes e Alto Douro (UTAD), Quinta de Prados, 5000-801, Vila Real, Portugal

⁸CECAV, Centro de Ciencia^ Animal e Veterinaria, Universidade de Tras-os-Montes e Alto Douro (UTAD), Quinta de Prados, Vila Real, 5000-801, Portugal

⁹Departamento de Patologia e de Imunologia Molecular, Instituto de Ciencias^ Biomedicas de Abel Salazar (ICBAS), Universidade do Porto (UP), Rua de Jorge Viterbo Ferreira, n 228, Porto 4050-313, Portugal

¹⁰Instituto de Patologia e Imunologia Molecular da Universidade do Porto (IPATIMUP), Rua Dr. Roberto Frias s/n, 4200-465, Porto, Portugal

¹¹Instituto de Investigac,ao~ e Inovac,ao~ em Saude (i3S), Universidade do Porto (UP), Rua Alfredo Allen, Porto 4200-135, Portugal

¹²Instituto Politecnico de Leiria, UIS-IPL: Unidade de Investigac,ao~ em Saude da Escola Superior de Saude de Leiria, Portugal

¹³CDrsp - Centre for Rapid and Sustainable Product Development, Rua de Portugal 2430-028, Marinha, Grande, Portugal

¹⁴Department of Clinical and Biological Sciences, University of Turin, Turin 10126, Italy

¹⁵Neuroscience Institute of the Cavalieri Ottolenghi Foundation (NICO), Azienda Ospedaliero-Universitaria San Luigi Gonzaga, Regione Gonzole 10, Orbassano, 10043, Turin, Italy

Abstract: The therapeutic effect of three polyvinyl alcohol (PVA) membranes loaded with electrically conductive materials - carbon nanotubes (PVA-CNTs) and polypyrrole (PVA-PPy) - were tested in vivo for neuro-muscular regeneration after an axonotmesis injury in the rat sciatic nerve. The membranes electrical conductivity measured was 1.5×10^{-6} S/m, 579×10^{-6} S/m, and 1837.5×10^{-6} S/m, respectively. At week-12, a residual motor and nociceptive deficit were present in all treated groups, but at week-12, a better recovery to normal gait pattern of the PVA-CNTs and PVA-PPy treated groups was observed. Morphometrical analysis demonstrated that PVA-CNTs group presented higher myelin thickness and lower g-ratio. The tibialis anterior muscle, in the PVA-PPy and PVA-CNTs groups showed a 9% and 19% increase of average fiber size area and a 5% and 10% increase of the “minimal Feret’s diameter,” respectively. No inflammation, degeneration, fibrosis or necrosis were detected in lung, liver, kidneys, spleen, and regional lymph nodes and absence of carbon deposits was confirmed with Von Kossa and Masson-Fontana stains. In conclusion, the membranes of PVA-CNTs and PVA-PPy are biocompatible and have electrical conductivity. The higher electrical conductivity measured in PVA-CNTs membrane might be responsible for the positive results on maturation of myelinated fibers. VC 2017 Wiley Periodicals, Inc. J Biomed Mater Res Part A: 105A: 1267–1280, 2017.

Key Words: nerve regeneration, axonotmesis, polyvinyl alcohol, nerve-guides, carbon nanotubes, polypyrrole, functional analysis, morphometric analysis, neurogenic atrophy

INTRODUCTION

Peripheral nerve injury has attracted public attention because of the societal and economic burden it has caused due to restriction of functional recovery of the individuals. Mechanical, thermal, chemical, or ischemic factors can be responsible for peripheral nerve injuries which include secondary neurogenic muscle atrophy.^{1,2} The high costs associated to individuals' disability and morbidity motivated surgeons, clinicians, and scientists to improve the current therapy and even increase the neuro-muscular regeneration. For this purpose, the development of biomaterials and cell therapies are crucial to therapeutic success.

The sciatic nerve in rats is commonly used as a model for the study of peripheral nerve regeneration. When full peripheral nerve transection injuries (neurotmesis) occur, reconstructive surgical procedures are always necessary³ but in case of axonotmesis injuries the surgical procedures are not necessary although the use of biomaterials or cellular therapies may increase the regeneration rate and diminish the neurogenic muscular atrophy responsible for functional disabilities.^{1,4-6} However, this injury model is often used in pre-clinical validations of biomaterials or cell-based therapies as it is a very well-studied model.^{2,5,7-13}

The use of electrically conductive biomaterials to produce tube-guides is a promising therapeutic, especially when the neurotmesis injuries^{9,13,14} have a gap which invalidates an end-to-end suture. The use of tube-guides will also allow the delivery of cell therapies in axonotmesis and neurotmesis injuries. Polyvinyl alcohol (PVA) is a polymer used as a biomaterial due to its biocompatibility, non-toxic, non-carcinogenic, swelling properties, and bio-adhesive characteristics and it can be used as host material to increase the solubility as well as the mechanical strength of conductive materials. It is also approved by Food and Drug Administration.^{15,16} Poly(pyrrole) (PPy) and COOH-functionalized multiwall carbon nanotubes (MWCNTs) are two of the most studied electrical conductive materials for tissue engineering, including the peripheral nerve regeneration. Both materials have unique properties such as conductivity¹⁷ and can be incorporated in several synthetic biodegradable material, including the ones made of PVA matrix. In the present experimental work, the effect of three different PVA membranes in nerve regeneration after a standard axonotmesis lesion in the rat sciatic nerve was studied. The study included simple PVA membranes, and those produced with

matrix of PVA loaded with MWCNTs (PVA-CNTs) and PPy (PVA-PPy).¹⁷ The use of the sciatic nerve axonotmesis injury model was chosen for validation of the best PVA composition to be used in a more serious lesion of neurotmesis. The importance of those composites is based on the hypothesis that such composites can be used to host the growth of resident cells and that electrical stimulation can be applied directly to cells through the composite, which proved to be beneficial in many regenerative strategies.¹⁸ Many studies have demonstrated that the chemical composition of the

local nerve injury environment is crucial for nerve regeneration including the presence of growth factors.¹⁹ The association of biomaterials that not only have a positive effect on peripheral nerve regeneration but are also capable of carrying or supporting a cellular system responsible for orchestrating this environment, has been recently demonstrated by our research group.^{1,5,7-9,11,13,20-23} The morphological

evaluation of the muscle tibialis anterior (TA) regeneration after the treatment of an axonotmesis injury with these three different membranes permitted the evaluation of neuromuscular recovery (and the neurogenic atrophy), and to correlate with the functional and morphological recoveries of the injured sciatic nerves.² The morphological assessment of the regenerated sciatic nerve and TA muscle was combined with functional evaluation during the healing period of 12 weeks which included the Withdrawal Reflex Latency (WRL) for the nociception function, the Extensor Postural Thrust (EPT) for determination of the motor deficit, the sciatic functional index (SFI) and the static sciatic index (SSI) and kinematic analysis of the ankle joint angle at the four selected instants of the stance phase: Initial Contact (IC),

Opposite Toe Off (OT), Heel Rise (HR), and Toe-Off (TO).^{1,2,5,7-9,11,20-22} The TA muscle morphometric analysis

was appropriate for the evaluation of nerve regeneration and subsequent muscle's reinnervation. The results obtained demonstrated the positive effect of using electrically conductive tube-guides, especially the PVA-

CNTs, to promote nerve regeneration and limit the neurogenic atrophy of the regional innervated muscles usually observed after serious nerve injuries and prolonged healing periods.

MATERIAL AND METHODS

Biomaterial membranes design and preparation Synthetic biodegradable membranes of PVA (Aldrich, Mowiol 10–98), PVA loaded with COOH-functionalized MWCNTs (Nanothinx, NTX5, MWCNTs 97% - COOH) (PVA-CNTs

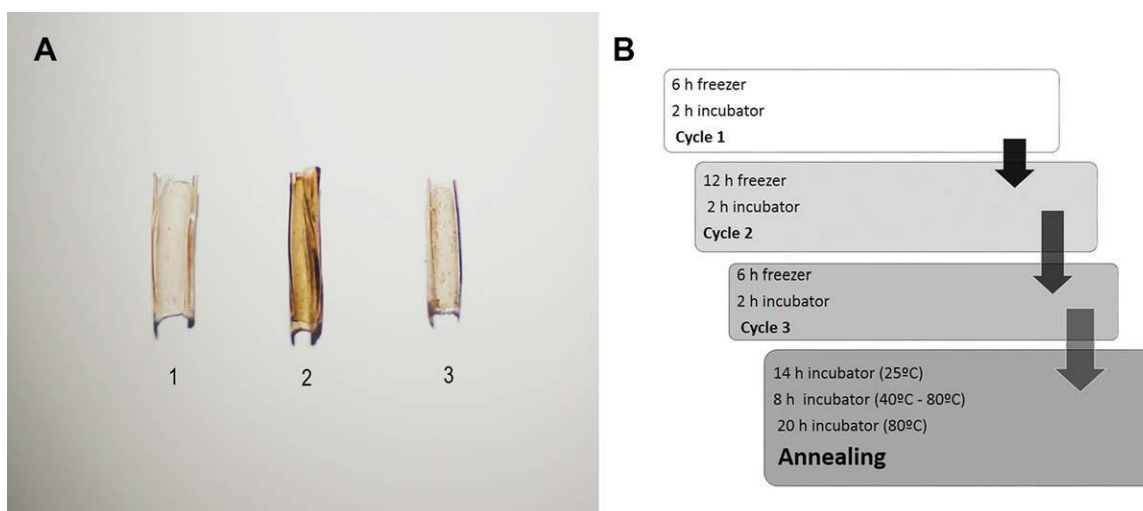


FIGURE 1. Synthetic biodegradable tube-guides/membranes of PVA (1), PVA loaded with COOH-functionalized MWCNTs (PVA-CNTs) (2), and PVA loaded with PPy (PVA-PPy) (3), used to wrap the sciatic nerve with a standardized axonotmesis injury (A). Schematic representation of the freezing/thawing process and the annealing treatment used for PVA, PVA-CNTs, and PVA-PPy membranes preparation (B).

membranes), and PVA loaded with PPy (Aldrich, 10–40 S/cm

of conductivity) (PVA-PPy membranes) were prepared according to Gonçalves et al. and Ribeiro et al.^{13,24} Briefly, applying

a casting technique using a silicone mould, a PVA aqueous solution 15% (w/v), a PVA aqueous solution 15% (w/v) supplemented with 0.05% of COOH-functionalized MWCNTs and a PVA aqueous solution 15% (w/v) supplemented with a 0.05% of PPy were prepared. The membranes were produced

by freezing/thawing cycles as described in Ribeiro et al. and Gonçalves et al.^{13,24} Gamma-radiation was used as sterilization

method and the membranes were hydrated in a sterile saline solution during 2 h before microsurgical application in the rat axonotmesis injuries (Fig. 1). Membranes physical - chemical characterization included electrical conductivity assessment, Differential Scanning Calorimetry (DSC) and enthalpy determination (DH), Fourier Transform Infrared Spectroscopy (FTIR), X-Ray Diffraction (XRD), Scanning Electronic Microscopy (SEM), and wettability determination, and the results were published elsewhere.^{13,24}

Surgical procedure

All the animal testing procedures were in conformity with the Directive 2010/63/EU of the European Parliament and with the approval of the Veterinary Authorities of Portugal in accordance with the European Communities Council Directive of November 1986 (86/609/EEC). Humane endpoints were always followed in accordance to the OECD Guidance Document on the Recognition, Assessment and Use of Clinical Signs as Humane Endpoints for Experimental Animals Used in Safety Evaluation (2000). All surgeries were performed by a veterinary surgeon of the research team with Felasa – Category C accreditation for animal experimentation. Adult male Sasco Sprague Dawley rats (Charles River Laboratories, Barcelona, Spain) weighing approximately 250–300 g, divided in four groups of seven animals each, were used. All animals were housed in a temperature and humidity controlled room with 12–12 h light/dark cycles, two animals per cage

(Polycarbonate cage type 3), and were allowed normal cage activities under standard laboratory conditions. The animals were fed with standard chow and water ad libitum. The anesthetic protocol used and the surgery techniques performed were the ones described previously elsewhere.²⁵⁻²⁷ A stand-

ardized crush injury was performed (axonotmesis) using a non-serrated clamp (manufactured by the Institute of Industrial Electronic and Material Sciences, University of Technology, Vienna, Austria) exerting a constant force of 54 N, for a 30 s period to create a 3 mm long crush injury, 10 mm above the bifurcation into tibial and common peroneal nerves. The

starting diameter of the sciatic nerve was about 1 mm, flattening during the crush to 2 mm.²⁵⁻²⁷ (Fig. 2). Four experimental

groups were studied. In groups 1 to 3, the sciatic nerve crush injury was wrapped by membranes: in group 1 the crush nerve was wrapped with a PVA membrane (group 1, PVA), in group 2, the crushed nerve was wrapped with a PVA membrane loaded with 0.05% (% w/v) of COOH-functionalized MWCNTs (group 2, PVA-CNTs), in group 3 the crushed nerve was wrapped with a PVA membrane loaded with Ppy 0,05% (% w/v) (group 3, PVA-PPy) and in group 4 the axonotmesis was performed without any additional procedure (group 4, Control) (Fig. 2).

Functional assessment

After standardized axonotmesis injury and sciatic nerve microsurgical reconstruction using the developed scaffolds, a follow-up consisting of the measurement of functional parameters important to evaluate the regeneration process during the healing period was performed. Animals have been tested pre-operatively (week-0), every week until week-8, and then every 2 weeks until the end of follow-up time (12 weeks). The ankle kinematics analysis was carried out prior nerve injury, and at week-12 of follow-up time, in the following experimental groups: PVA, PVA-CNTs, PVA-PPy, and Control. Animals were gently handled, and tested in a quiet environment to minimize stress.

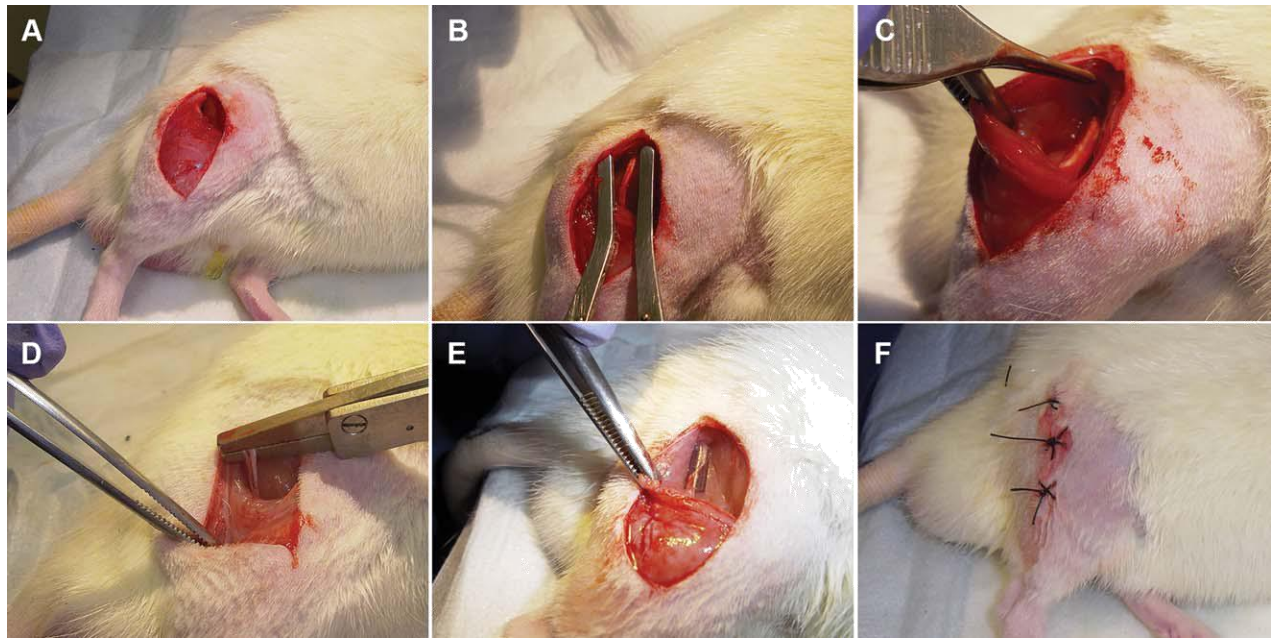


FIGURE 2. Photographs of the surgery procedure. Incision in the skin from the greater trochanter to the mid-half distally followed by a muscle splitting incision (A) and the right sciatic nerve was exposed (B). After sciatic nerve mobilization, a standardized crush injury was performed (axonotmesis) using a non-serrated clamp (C, D). The sciatic nerve crush injury was wrapped by different PVA electrical conductive materials (E). Skin suture (F).

Motor performance and nociceptive function. Motor performance and nociceptive function were evaluated by measuring EPT and WRL, respectively. To assess the nociceptive WRL, the hotplate test was modified as described by Masters et al.²⁸ The animal is wrapped in a surgical towel above its waist and then positioned to stand with the affected hind paw on a hot plate, at 56°C, and with the other on a room temperature plate. WRL is defined as the time elapsed from the onset of hotplate contact to withdrawal of the hind paw and meas-

ured with a stopwatch. Normal animals withdraw their paws from the hotplate within 4.3 s or less.^{4,8,11,22,29,30} The affected

limbs were tested 3 times, with an interval of 2 min between consecutive tests to prevent sensitization, and the three latencies were averaged to obtain a final result.³¹ If there was no paw withdrawal after 12 s, the heat stimulus was removed to

prevent tissue damage, and the animal was assigned the maximal WRL of 12 s.^{25,32}

The EPT was originally proposed by Tralhammer et al.^{33,34} as a part of the neurological recovery evaluation in

the rat after sciatic nerve injury. For this test, the entire body of the animal, with exception of the hind-limbs, is wrapped in a surgical towel. EPT is induced by supporting the animal by the thorax and lowering the affected hind-limb toward the platform of a digital balance. As the animal is lowered to the platform, it extends the hind-limb, anticipating the contact made by the distal metatarsus and digits. The force in grams

(g) applied to the digital platform balance is recorded. The same procedure is applied to the contra-lateral, unaffected limb. For the EPT test, the affected and normal limbs are tested three times, with an interval of 2 min between consecutive tests, and the three values are averaged to obtain a final result. The normal (unaffected limb) EPT (NEPT) and

experimental EPT (EEPT) values are incorporated into an equation [Eq. (1)] to derive the percentage of functional deficit, as described in the literature.^{4,8,21,30,33,34}

$$\% \text{ Motor deficit} = \frac{5 \times \delta \text{NEPT} + 2 \text{EEPT} - \text{NEPT}}{3} \times 100 \quad (1)$$

Sciatic functional index and static sciatic index. For SFI, animals are usually tested in a confined walkway that they cross, measuring 42-cm long and 8.2-cm wide, with a dark shelter at the end. Several measurements must be taken from the footprints: (i) distance from the heel to the third toe, the print length (PL); (ii) distance from the first to the fifth toe, the toe spread (TS); and (iii) distance from the second to the fourth toe, the intermediary toe spread (ITS). In the SSI evaluation only the parameters TS and ITS, are measured. For SFI and SSI, all measurements are taken from the experimental (E) and normal (N) sides. Prints for measurements are chosen at the time of walking based on pre-clarity, clear, and completeness of footprints. The mean distances of three measurements are used to calculate the following factors (dynamic and static): SFI is calculated as described by Bain et al.³⁵ according to the following Eq. (2):

$$\begin{aligned} \text{SFI} = & \frac{5 \times \delta \text{EPL} - \text{NPL} + \text{NPL}}{1} \times \frac{109.5 \times \delta \text{ETS} - \text{NTS}}{8.85} \\ & + \frac{13.3 \times \delta \text{EIT} - \text{NIT}}{8.85} + \frac{238.3 \times \text{PL}}{109.5} \\ & + \frac{3 \times \text{TS}}{13.3} + \frac{3 \times \text{ITS}}{13.3} - 8.8 \end{aligned} \quad (2)$$

SSI is calculated as described by Bervar et al.³⁶ according to the following Eq. (3):

$$\text{SSI} = \frac{5108.4 \times \text{TS} + 131.85 \times \text{ITF}}{5.49} \quad (3)$$

For SFI and SSI, an index score of 0 is considered normal and an index of 2100 indicates total impairment. When no footprints are measurable, the index score of 2100 is given. In each walking track three footprints should be analyzed by a single observer, and the average of the measurements is used in SFI calculations.

Kinematic analysis. Ankle kinematics analysis was carried out prior nerve injury, and at week-12 of follow-up time, in the following experimental groups: PVA, PVA-CNTs, PVA-PPy, and Control. Animals walked on a Perspex track with length, width and height of 120, 12, and 15 cm, respectively. To ensure locomotion in a straight line, the width of the apparatus was adjusted to the actual animal size during the experiments. The animals' gait was video recorded at a rate of 300 Hz images per second (Casio Exilim PRO EX-F1, Japan). The camera was positioned at the track half-length where gait velocity was steady, and 1 m distant from the track obtaining a visualization field of 14 cm wide. The video images were stored in a computer hard disk for later analysis using an appropriate software APASVR (Ariel Performance Analysis System, Ariel Dynamics, San Diego). Two-dimensional biomechanical analyses (sagittal plane) was carried out applying a two-segment model of the ankle joint, adopted from the model first developed by Refs. 37 and 38. The animals' ankle angle was determined using the scalar product between a vector representing the foot and a vector representing the lower leg. With this model, positive and negative values of position of the ankle joint (θ) indicate dorsiflexion and plantarflexion, respectively. For each step

cycle, the following time points were identified: IC, OT, and HR and TO.^{22,32,38} and were time normalized for 100% of step cycle. The normalized temporal parameters were averaged over all recorded trials. A total of six walking trials for each animal with stance phases lasting between 150 and 400 ms were considered for analysis, as this corresponds to the animal's normal walking velocity (20–60 cm/s).^{22,37,38}

Morphological analysis and histopathology Morphological assessment of nerve. Nerve samples (10-mm-long

sciatic nerve segments distal to the crush site and from un-operated controls) were processed for quantitative morphometry of myelinated nerve fibers. Fixation was carried out using 2.5% purified glutaraldehyde and 0.5% sac-carose in 0.1 M Sorensen phosphate buffer for 6–8 h and resin embedding was obtained following Glauerts' procedure. Series of 2-mm thick semi-thin transverse sections were cut using a Leica Ultracut UCT ultramicrotome (Leica Microsystems, Wetzlar, Germany) and stained by Toluidine blue. Stereology was carried out on a DM4000B microscope equipped with a DFC320 digital camera and an IM50 image manager system (Leica Microsystems, Wetzlar, Germany). Systematic random sampling and D-disector were adopted using a protocol previously described.^{39,40} Total number of myelinated fibers, axon size, myelin thickness, and g-ratio were evaluated.

Morphological assessment of muscle. At termination of the functional testing performed in this study, TA muscles of all the axonotmesis and TA muscles without lesion (Pre crush group) were collected, and the tissue samples were fixed in 10% buffered formalin, routinely processed, dehydrated and embedded in paraffin wax. Consecutive 3 μ m transverse sections from the mid-belly of each muscle were cut and stained with haematoxylin and eosin (HE) and kept for morphometry and determination of degree of atrophy. For the morphometric analysis, an unbiased sampling procedure was applied. The muscle fibers' cross section area and "minimal Feret's diameter" which is the minimum distance of parallel tangents at opposing borders of the muscle fiber, were evaluated from the cross sections using the ImageJVC software (NIH) which allowed to apply this set of individual fiber measurements. A minimum of 1000 skeletal muscle fibers was measured from each group. This assessment was performed by two independent operators. Each one of the operators blindly and randomly measured an average of 50 fibers in each section. Images were acquired using a NikonVR microscope connected to a Nikon^{VR} digital camera DXM1200, at low magnification (1003) under the same conditions that were used to acquire a reference ruler.

Histology of internal organs. At the end of the study, all animals were subjected to a complete necropsy examination to evaluate the presence of possible internal anomalies and/ or injuries. Spleen, liver, kidney, lung, and lymph nodes were collected, weighed, and submitted to histological examination to identify putative related microscopic alterations such as inflammation, degeneration, or accumulation of biological material. Tissues were fixed in 10% neutral buffered formalin and embedded in paraffin wax. Three consecutive sections of 3 μ m were made, one being stained with hematoxylin-eosin (HE) and the others were used for histochemical staining. Microscopically, massive carbon deposits generally appear as well-recognized anthracotic black pigment, especially in the lung. A recent report described that some types of CNTs may appear as small punctuated intracellular accumulations in the Kuepfer cells (liver) and in the intermediate zone of the spleen, when intravenously administered.⁴¹ Special stains such as Von Kossa (VK - method that demonstrates phosphates and carbonates) and Masson-Fontana (MF - method used for distinguish carbon deposits from melanin) were performed to exclude the presence of these substances in the different tissues under study concerning the experimental group of PVA-CNTs.

Statistical analysis

For sciatic nerve functional analysis, a mixed model repeated measures ANOVA was used to test for differences across time and sciatic nerve treatment. Sphericity was assessed by Mauchly's test and Greenhouse-Geisser degrees of freedom correction was used in cases sphericity could not be assumed or when corrected p-values were below the accepted level of significance ($p < 0.05$). Tukey's HSD test was used for pairwise comparisons. Ankle kinematics data

TABLE I. Measurements of the In Vitro Electrical Conductivity of the Three Membranes: PVA, PVA-PPy, and PVA-CNTs Used in the Rat Sciatic Nerve In Vivo Model

Sample	Conductivity (S/m) $\times 10^6$
PVA 15%	1.461/20.49
PVA 15% 1PPy 0.025%	5791/20.607
PVA 15% 1CNTs 0.05% COOH	12501/20.707

were analyzed with One-way ANOVA. All data are presented as mean and standard deviation (SD), unless otherwise stated. These statistical tests were carried out with IBM SPSS Statistics Version 19. For stereology, statistical comparisons of quantitative data were subjected to one-way ANOVA test, followed by pairwise comparisons using Tukey's HSD test. Statistical significance was established as $p < 0.05$. Stereological data were analyzed using the software using the SPSS version 19.0 (SPSS, Chicago, IL). For muscle morphometry, statistical analysis was performed using the SPSS version 19.0 (SPSS, Chicago, IL). Results are presented as mean \pm SEM. Multiple comparisons between groups were performed by one-way ANOVA supplemented with Tukey's HSD post hoc test. Differences were considered statistically significant at $p < 0.05$.

RESULTS

Biomaterial characterization

The three different tube-guides of PVA were physicochemical characterized (PVA, PVA-CNTs, and PVA-PPy). All the results were in agreement with the findings previously reported.^{13,24} The electrical conductivity achieved for the three different membranes (PVA, PVA-CNTs, and PVA-PPy) was 1.56×10^6 S/m, 5796.6×10^6 S/m, and 1837.5×10^6 S/m, respectively (Table I). In light of the conductivity results, the three membranes (simple PVA, PVA loaded with 0.05% (% w/v) of COOH-functionalized CNTs and PPy) compositions were chosen for in vivo application in the rat sciatic nerve axotomy and neurotomy injury models.^{13,24} The thermal characteristics of simple PVA and loaded PVA materials (PVA-CNTs and PVA-PPy) were examined by DSC and Enthalpy of Fusion (DH) was calculated, and the percentage of crystallinity was near 7.4% for all analyzed nerve membranes. FTIR analysis of the bands identified for PVA loaded with COOH-functionalized CNTs (PVA-CNTs) were similar to the bands detected for simple PVA. For PVA loaded with PPy (PVA-PPy), new bands appeared at 1313 cm^{-1} (C-N stretching vibration in the ring) and 1170 cm^{-1} (C-H in-plane deformation). Compared with simple PVA, the other membranes showed inferior intensity of the peaks, especially between 2237 and 2380 cm^{-1} .^{13,24} Considering the XRD analysis previously performed, the broad peak observed at $2\theta = 20.8^\circ$ corresponded to a typical diffraction peak of PVA, and it could be also observed in all membranes. Near $2\theta = 26.8^\circ$ a broad scattering peak appeared for the tube loaded with PPy (PVA-PPy), and it was an indication of the presence of PPy as supported in literature.^{13,42} Both PVA and PVA loaded with PPy (PVA-PPy) when analyzed by SEM exhibited similar surface

appearance. Conversely, the PVA loaded with COOH-functionalized CNTs (PVA-CNTs) showed a rougher surface as expected due to the presence of CNTs on PVA matrix, with oriented features.^{13,24} This characteristic was determinant on the choice of this biomaterial to be associated to the MSCs (PVA-CNTs-MSCs group) in sciatic nerve neurotmesis injury reconstruction with functional and morphologic positive regenerating outcomes.^{13,24} The wettability analysis showed a hydrophilic behavior for the three biomaterials used for tube-guide tested, also the three materials showed negative zeta potential being the PVA the most negative surface (24.97 mV)^{13,24} (Table I, Fig. 1).

Functional assessments of re-innervation

Immediately after axotomy, the crushed areas of all sciatic nerves were flattened but nerve continuity was preserved. Following crush injury, a complete sciatic nerve paralysis was observed in all experimental animals. All animals survived without auto-mutilation and normal wound healing. All rats were evaluated pre-operatively (week-0) and every week during 8 weeks and then at week-10 and week-12, when the animals were sacrificed for morphological analysis of nerve and TA muscles.

Motor deficit and nociceptive function. Motor deficit - extensor postural thrust (EPT). Values of percentage of functional deficit (%), were obtained by performing the EPT test, preoperatively (week-0), and every week during 8 weeks and then at weeks 10 and 12 (Fig. 3). In the week following sciatic nerve crush, motor deficit was severe and compatible with almost complete loss of postural extensor thrust response in the affected side (Fig. 3). The mixed two-way ANOVA results indicate a significant effect of time for motor deficit values [$F_{(9,216)} 5 22.379$; $p < 0.001$] but no time versus group interaction or group effects. The simple contrasts showed that significant improvement in motor deficit could be noticed from week-3 post-injury onwards. One-way ANOVA showed that no differences between the groups existed in motor deficit scores before sciatic nerve crush. At week-12, the three experimental groups (PVA, PVA-CNTs, PVA-PPy) presented a residual motor deficit of 0.16 60.31, 0.10 6 0.41, and 0.16 6 0.59, respectively, The individual variability between animals of the same experimental group is evidenced due to the subjectivity of the test, but it can be concluded that no differences between the experimental groups existed in motor deficit scores at week-12 sciatic nerve crush by one-way ANOVA (Fig. 3).

Nociception function – withdrawal reflex latency (WRL). Values in seconds were obtained by performing the WRL test, preoperatively (week-0), and every week during 8 weeks and then at weeks 10 and 12. A severe loss of thermal sensitivity in the affected paw could be noticed immediately after sciatic nerve crush (Fig. 4). From such acute thermal and pain sensitivity loss, a steady recovery of the withdrawal response to thermal stimulus occurred throughout the following weeks such as mixed two-way ANOVA could find a significant effect of time [$F_{(9,216)} 5 6.072$; $p < 0.001$] but no time versus group

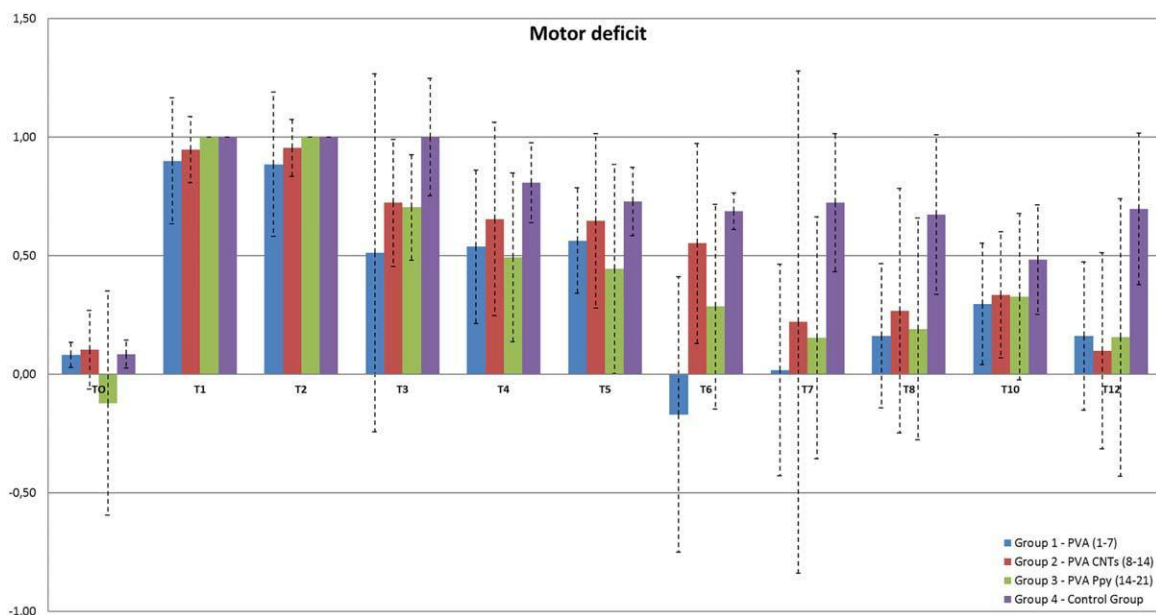


FIGURE 3. Graphical representation of the mean values of Motor Deficit obtained performing EPT test. This

test has been performed preoperatively (week-0), and every week during 8 weeks and then at week-10 and week-12. Results are presented as mean and standard error of the mean (SEM). N corresponds to the number of rats within the experimental group (N 57).

interaction or group effects. According to simple contrasts testing, significant improvement in the latency for paw withdrawal took place following week-4. One-way ANOVA showed that no differences between the groups existed in WRL times before sciatic nerve crush. At week-12, the three experimental groups (PVA, PVA-CNTs, PVA-PPy) presented a withdrawal response to thermal stimulus near normal values of 4.3s (5.26 ± 0.15, 5.34 ± 61.43, and 5.28 ± 61.43, respectively). The individual variability between animals of the same experimental group is evidenced once again by the subjectivity of the test which emphasizes the need to perform kinematics analysis of the gait of the treated rats. It can be concluded that no differences between the experimental groups existed considering the nociceptive function scores at week-12 sciatic nerve crush by one-way ANOVA (Fig. 4).

Sciatic functional index and static sciatic index. Scores of SSI drop severely immediately after sciatic nerve crush and thereafter showed a progressive recovery (Fig. 5). Therefore, two-way ANOVA found a significant time effect

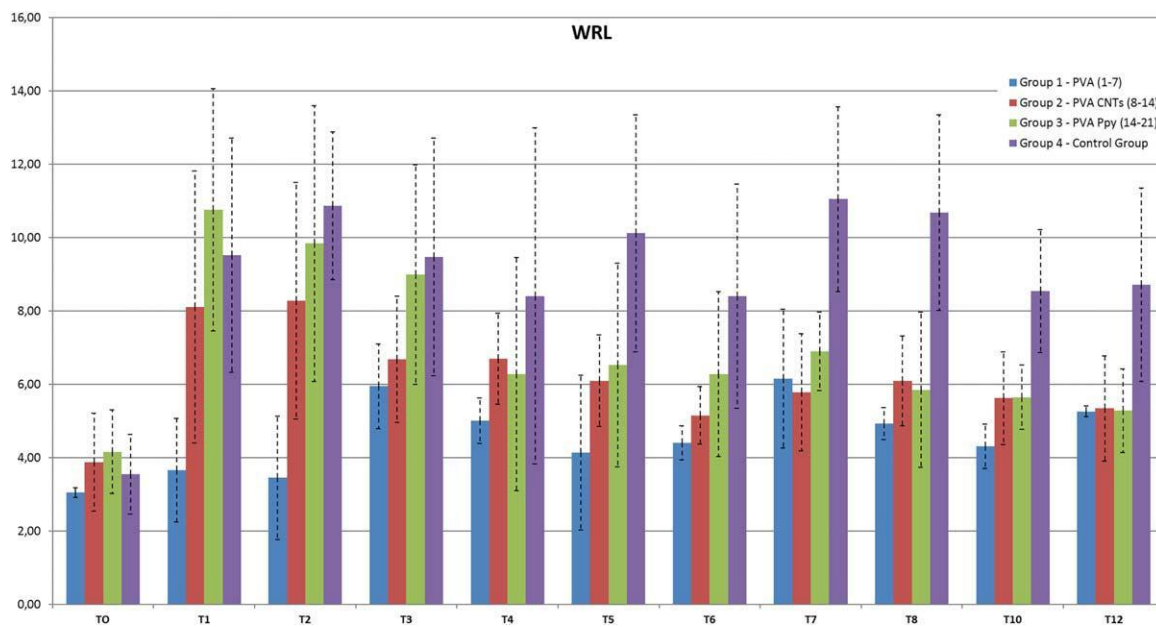


FIGURE 4. Graphical representation of the mean values in seconds (s) obtained performing WRL test to evaluate the nociceptive function. This test has been performed pre-operatively (week-0), and every week during 8 weeks and then at week-10 and week-12. Results are presented as mean and standard error of the mean (SEM). N corresponds to the number of rats within the experimental group (N 57).

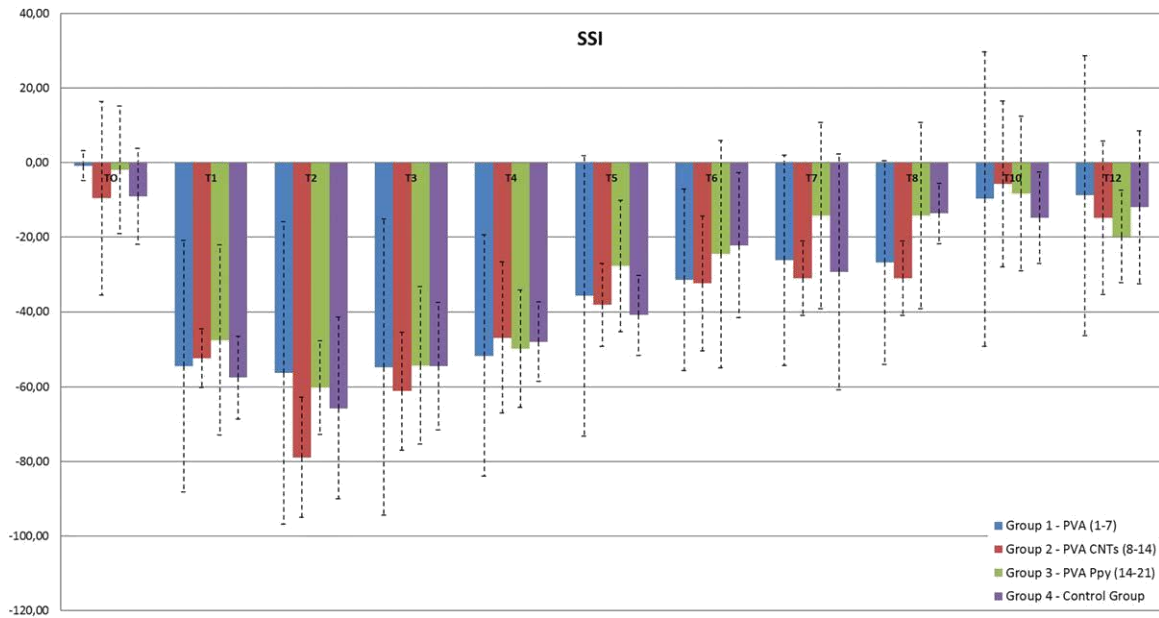


FIGURE 5. Graphical representation of the mean values of Static Sciatic Function (SSI) measured pre-operatively (week-0), and every week during 8 weeks and then at week-10 and week-12. An index score of 0 is considered normal and an index of 100 indicates total impairment. The measurements of the TS, and the ITS, were taken from the experimental (E) and normal (N) sides. Results are presented as mean and standard error of the mean (SEM). N corresponds to the number of rats within the experimental group (N 5 7).

[$F_{(9,189)} 519.218$; $p < 0.001$] but once again without time versus group interaction and group effects. The recovery of SSI scores started to be consistently significant from week-

5. One-way ANOVA showed that no differences between the groups existed in SSI scores before sciatic nerve crush. At week-12, the three experimental groups (PVA, PVA-CNTs, PVA-PPy) presented SSI scores of 28.81 \pm 37.50, 21.79 \pm 20.65, and 219.80 \pm 12.39, respectively (Fig. 5).

Scores of SFI measured in the week following sciatic nerve crush reached very low values, indicating severe loss of sciatic nerve function (Fig. 6). From this time point, SFI scores showed a very robust recovery so that two-way ANOVA found a significant time effect [$F_{(9,189)} 576.708$; $p < 0.001$], with recovery starting as soon as week-2. Again, no time versus group and group effects existed. Likewise, no differences between the groups could be found before

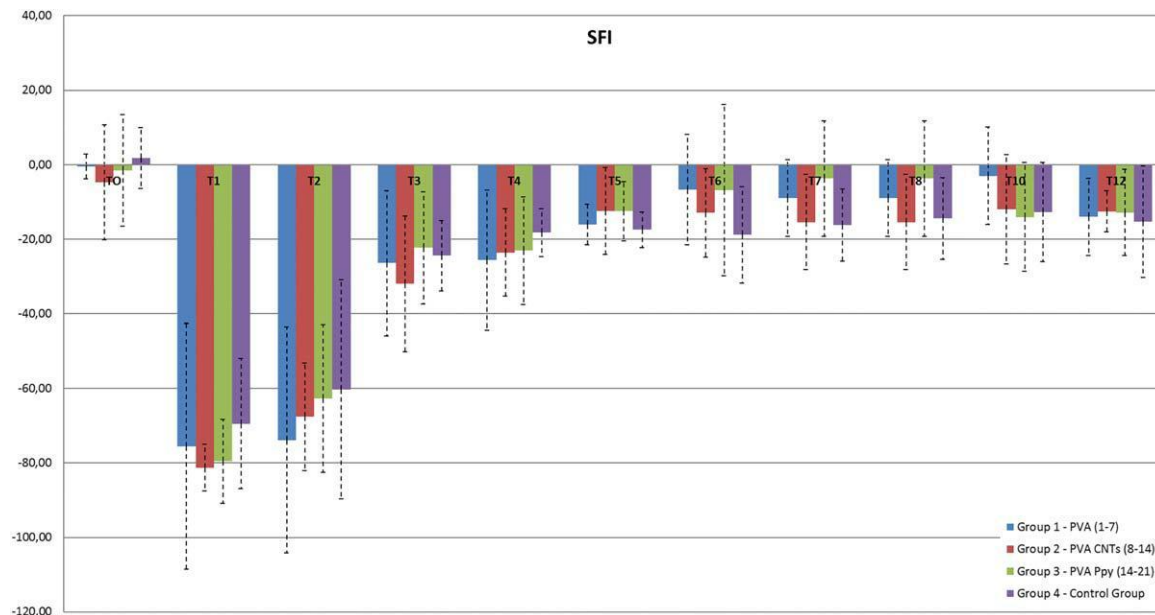


FIGURE 6. Graphical representation of the mean values of Sciatic Function Index (SFI) measured pre-operatively (week-0), and every week during 8 weeks and then at week-10 and week-12. An index score of 0 is considered normal and an index of 100 indicates total impairment. The measurements of the PL, the toe spread (TS), and the ITS, were taken from the experimental (E) and normal (N) sides. Results are presented as mean and standard error of the mean (SEM). N corresponds to the number of rats within the experimental group (N 57). sciatic nerve crush. At week-12, the three experimental groups (PVA, PVA-CNTs, PVA-PPy) presented SFI scores of 214.01 610.40, 212.55 65.57, and 212.86 611.56, respectively (Fig. 6).

Kinematic analysis. For kinematic analysis, measures of ankle joint angle at the four selected instants of the stance phase (IC, OT, HR, and TO) were collected before sciatic nerve injury and at the end of 12-weeks recovery period (N 57) (Table II, Fig. 7). At 12-weeks post-injury, ankle kinematics improved in every group approaching its pre-injury pattern. At this time point, ankle angle was similar at IC and it was similar for every group of animals. However, at OT and HR subtle differences between groups in ankle angle could be devised, with animals treated with conductive membranes revealing slightly abnormal ankle kinematics, comparing with the control and uninjured animals ($p < 0.05$). At TO normal ankle angle, values were registered for all groups with the relative exception of the PVA group for which the ankle seemed somewhat excessive at this instant of the gait cycle, particularly when comparing with uninjured animals ($p = 0.065$).

Morphological analysis and histopathology Histo-morphometry of the regenerated sciatic nerve. Histological analysis on Toluidine Blue stained semi-thin sections showed that nerve fiber regeneration occurred in all repaired nerves 12 weeks after surgery [Fig. 8(A-C)] with a micro-fasciculation typical of regenerated nerve fibers. Morphometrical analysis [Fig. 8(D)] allowed to compare the three groups in terms of number of myelinated fibers, axon diameter and myelin thickness. Moreover, g-ratio was also calculated to better appreciate maturation of myelinated fibers. The PVA group (N 57), presented a total number of myelinated fibers of 16,596 61737, axon diameter (d) of 2.95 60.17, fiber diameter (D) of 3.56 60.21, myelin thickness (M) of 0.31 60.02, ratio axon diameter and fiber diameter (d/D, g-ratio) of 0.82 60.01. The PVA-CNTs regenerated nerves (N 57) presented a total number of myelinated fibers of 16,049 62442, axon diameter (d) of 2.98 60.18, fiber diameter (D) of 3.71 60.20, myelin thickness (M) of 0.37 60.02, ratio axon diameter and fiber diameter (d/D, g-ratio) of 0.79 60.01. The PVA-PPY regenerated nerves (N 57) presented a total number of myelinated fibers of 22,588 63596, axon diameter (d) of 3.03 60.10, fiber diameter (D) of 3.70

60.12, myelin thickness (M) of 0.33 60.01, ratio axon diameter and fiber diameter (d/D, g-ratio) of 0.81 60.00 [Fig. 8(D)]. The results described showed no differences in terms of number of myelinated fibers and axon diameter between the three groups, but it is possible to appreciate statistically significant differences between PVA and PVA-CNTs groups in the evaluation of myelin thickness (*p 0,05) and g-ratio (**p 0,01) and between PVA-PPY and PVA-CNTs as regards g-ratio (d/D) evaluation (*p 0,05). The decrease of g-ratio when axon diameter is similar, is an index of a better maturation of myelinated fibers [Fig. 8(D)].

TABLE II. Ankle Kinematics – Values Were Obtained Perform-ing Video Analysis at Week-12 of the Healing Period

Temporal Events	Group	Result
IC	Group 1 - PVA	20.10 6
	Group 2 - PVA1Ppy	4.25 67.45
	Group 3 - PVA1CNTs	6.12 65.46
	Pre crush	5.82 61.33
	Group 4 - Control	4.68 62.25
OT	Group 1 - PVA	9.84 7
	Group 2 - PVA1Ppy	14.84 65.08
	Group 3 - PVA1CNTs	11.11 64.64
	Pre crush	8.92 64.93
	Group 4 - Control	7.40 63.15
HR	Group 1 - PVA	22.88 64.83
	Group 2 - PVA1Ppy	22.57 8
	Group 3 - PVA1CNTs	16.97 68.45
	Pre crush	16.39 65.86
	Group 4 - Control	11.92 65.61
TO	Group 1 - PVA	11.43 9
	Group 2 - PVA1Ppy	215.93 63.09
	Group 3 - PVA1CNTs	21.62 68.04
	Pre crush	23.20 8
	Group 4 - Control	211.83 4

Results are presented as mean and standard deviation (SD) (N 5 7). For each step cycle, the following time points were identified: initial contact (IC), Opposite Toe off (OT), and Heel Rise (HR) and Toe-off (TO).

Morphological analyses of the TA muscle. Following 12 weeks of sciatic nerve crush, it was possible to observe by muscle morphometry that there was a significant difference ($p < 0.05$) in terms of fiber size between sciatic nerve with-out lesion (Pre crush), sciatic nerve with axonotmesis injury without surgical reconstruction (Control) and the treatment (PVA, PVA-PPy, and PVA-CNTs) groups. In the PVA-PPy treatment group, there was a 9% increase in terms of average fiber size area and a 5% increase in term of the “minimal Feret’s diameter,” when comparing to the untreated Control group (Fig. 9). In the PVA-CNTs treatment group, there was a 19% increase in terms of average fiber size area and a 10% increase in term of the “minimal Feret’s diameter,”

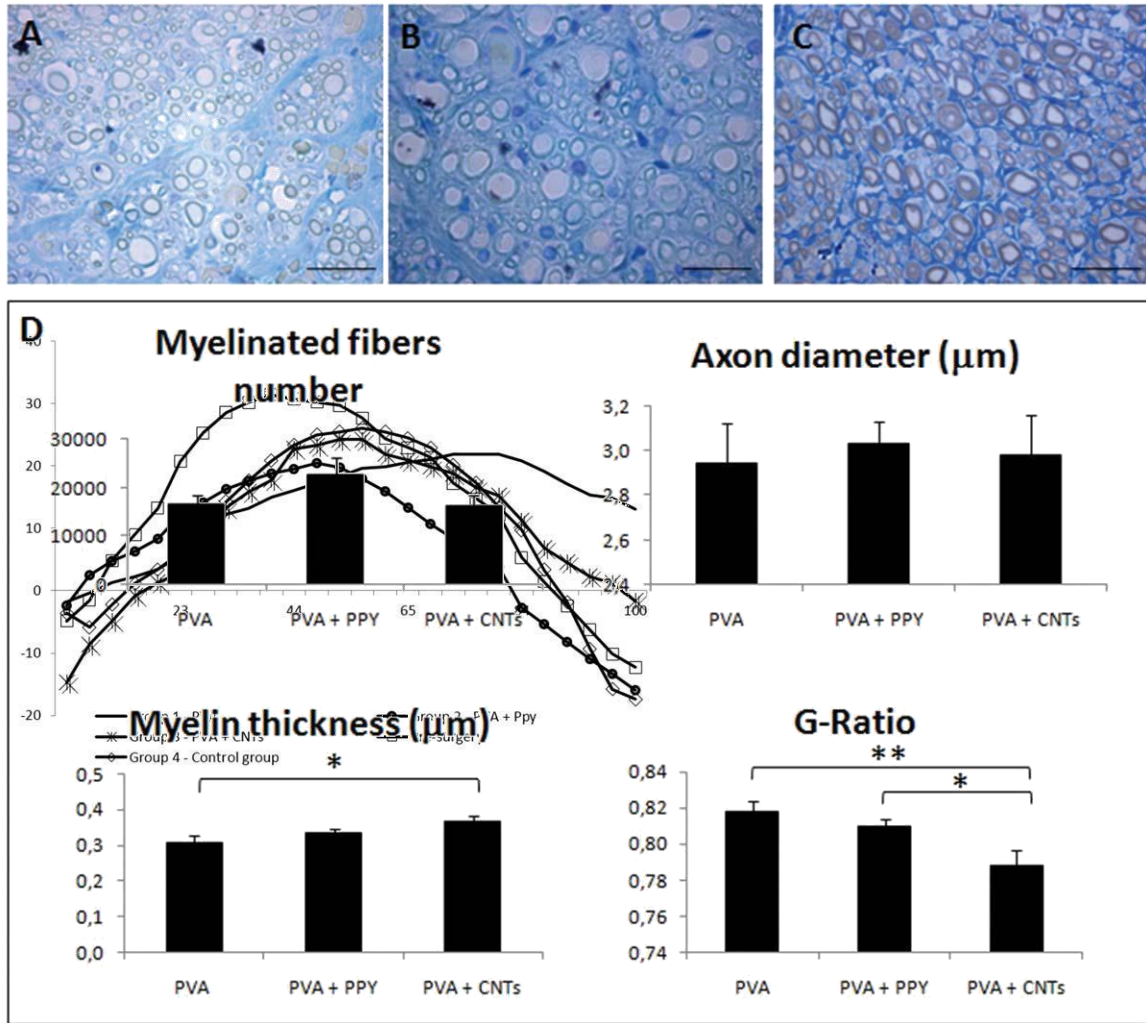


FIGURE 7. Kinematic plots in the sagittal plane for the ankle angle (θ) as it moves through the stance phase, during the transection injury study. The mean of each group is plotted.

FIGURE 8. Histological appearance of regenerated nerve fiber in the different groups of axonotmesis: PVA (A); PVA-PPY (B); PVA-CNTs (C). Mag-nification: 10003; scale bar 520 mm. Stereological quantitative assessment - total number of myelinated fibers, axon diameter, myelin thickness, ratio axon diameter and fiber diameter (d/D , g-ratio) of regenerated sciatic nerve fibers at week-12 after surgery. Values are presented as mean \pm 6 SEM. * $p < 0.05$; ** $p < 0.01$ (D).

when comparing to the untreated Control group. Opposite results were observed for the PVA group in which the mean fiber size area and “minimal Feret’s diameter” were significantly lower than the untreated group (17% and 9%, respectively) (Fig. 9).

Histology of internal organs. At the histological examination, no alterations compatible with images of inflammation, degeneration, fibrosis, or necrosis were detected in all animals from the three experimental groups (PVA, PVA-PPy, and PVA-CNTs). The negative results obtained with both Von Kossa and Masson-Fontana stains reinforced the absence of nanotubes and carbon deposits in all the organs in all animals from the experimental group of PVA-CNTs (Fig. 10).

DISCUSSION

The peripheral nervous system (PNS) establishes the connection between the central nervous system (CNS) and the peripheral structures, including the innervating of regional skeletal muscles. Innervation regulates skeletal muscle mass and muscle phenotype and changes in the muscles may contribute to functional deficit after nerve injury.² The neuro-muscular regeneration analysis is very important to evaluate new therapeutic approaches that will allow better functional recovery of the individuals, sometimes limited by the regional muscle atrophy and fibrosis. After injury, the functional recovery can be partially gained in the PNS because of the presence of Schwann cells (SCs), which are able to supply nutrient support, guide, and myelinate regenerating axons, and provide growth factors,⁵ where the Wallerian degeneration has a crucial role.^{2,5} After axonotmesis, spontaneous regeneration through the distal nerve stump can be expected but a total functional recovery is frequently not achieved. By reducing the healing period after axonotmesis, using several therapeutic strategies, and promoting the peripheral nerve regeneration, the secondary neurogenic muscle atrophy can be diminished, with improvement of the functional outcome.^{2,5} Experiments on peripheral nerve

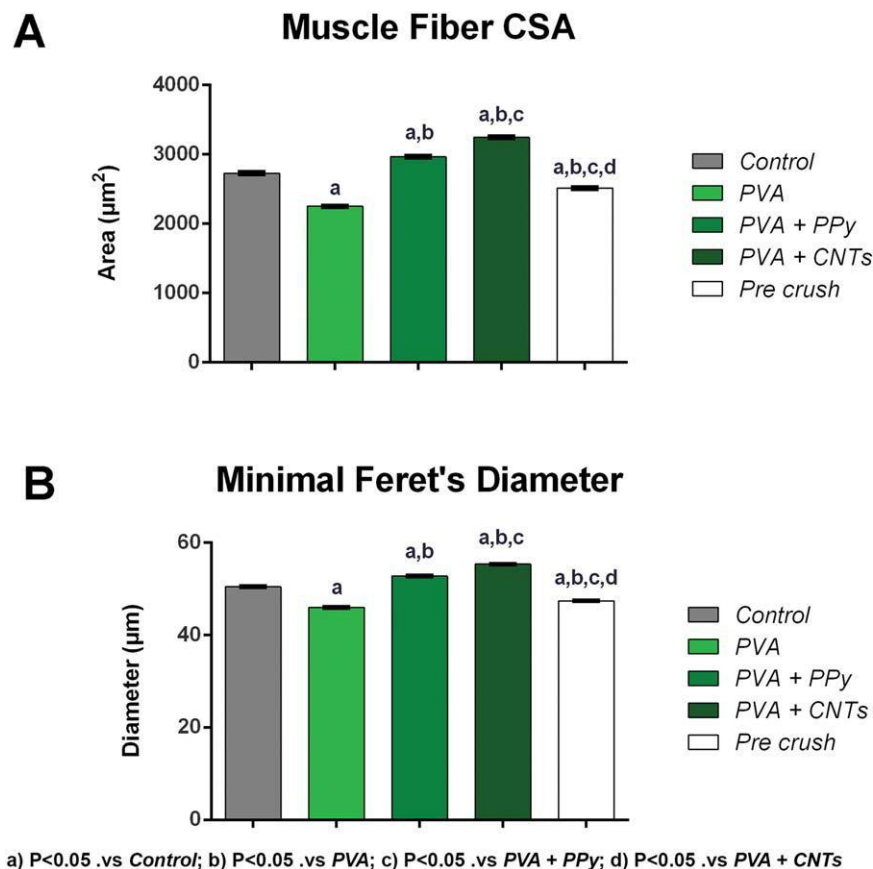


FIGURE 9. Graphical representation of the mean of area (A) and “minimal Feret’s diameter” (B) of Pre Crush, regenerated TA muscle fibers at week-12 after axonotmesis (untreated or Control) and axonotmesis

with the sciatic nerve enwrapped in different PVA membranes (PVA, PVA-PPy, and PVA-CNTs). Values are presented as mean \pm SEM.

regeneration^{5,29} are often performed on the rat sciatic nerve model⁴³ and the axonotmesis injury, conversely, is the most widely used in vivo model to test several biomaterials for tube-guide nerve fabrication and more recently, for cellular therapies that are applied in more serious nerve injuries like the neurotmesis.^{2,4,7-13,29,44}

In the present experimental work, it was studied the effect of three different PVA membranes in nerve regeneration after a

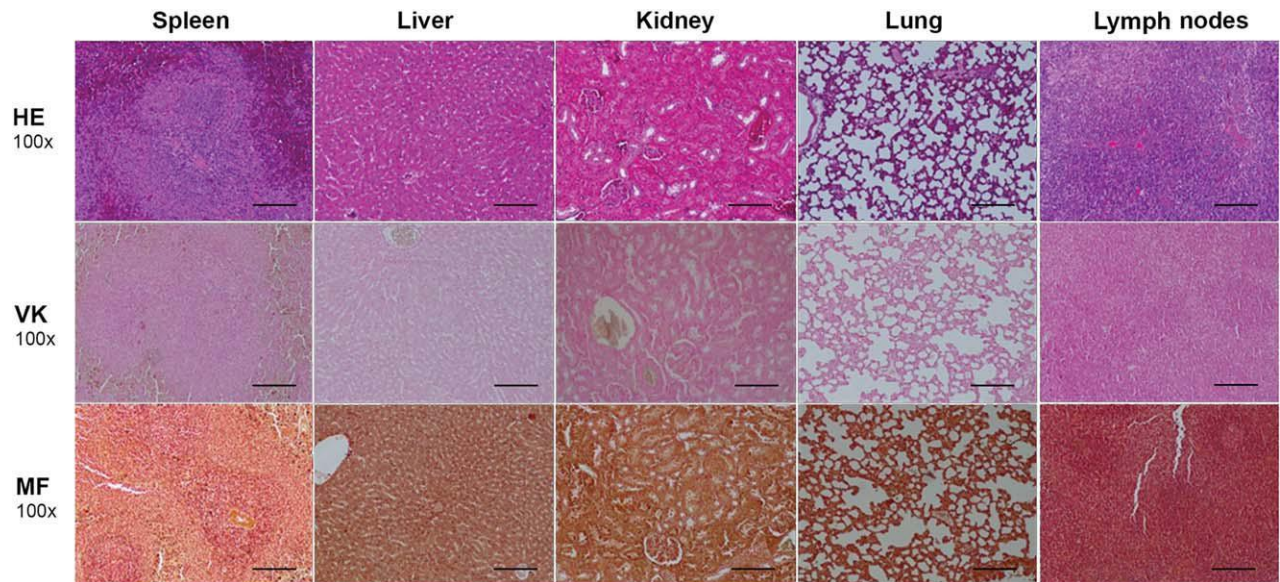


FIGURE 10. Histological analysis of spleen, liver, kidney, lung, and lymph nodes collected at week-12, from animals of the experimental group PVA-CNTs. Magnification: 1003; scale bar 510 mm. HE: hematoxylin-eosin; VK: Van-Kossa; MF: Masson Fontana staining.

standard axonotmesis lesion in the rat sciatic nerve: simple PVA, and those produced with a matrix of PVA loaded with MWCNTs (PVA-CNTs) and PPy (PVA-PPy). These last two types of membranes presented increased electrical conductivity when compared with the PVA membrane, which was considered as being an advantage for nerve regeneration.¹⁷ PVA is a biodegradable, water-soluble synthetic polymer that has been increasingly used in biomedical applications. PVA may mimic the regulatory characteristics of natural extracellular matrix (ECM) and ECM-bound growth factors.⁹ Its hemocompatibility and biocompatibility was previously confirmed when PVA was previously used by our research group in vascular grafting.⁴⁵ PVA was also previously evaluated in association with human MSCs (hMSCs) isolated from the umbilical cord (UC) Wharton's jelly. For this purpose, hMSCs were cultured on PVA membranes and it was proved the cytocompatibility and biointegration of the developed biomaterial associated to this cellular system when used in vivo in pre-clinical trials in ovine animal model⁴⁵ and rat neurotmesis sciatic nerve injury model.¹³ The polymers with electrical conductivity have attracted interest because they simultaneously display the physical and chemical properties of organic polymers and the electrical characteristics of metals which might improve the neuromuscular regeneration. The importance of those polymers is based on the hypothesis that such biomaterials can be used to host the growth of cells, and electrical stimulation can be applied directly to the cells, which proved to be beneficial in many

regenerative strategies, where neuromuscular regeneration is the one of the most promising areas.^{9,17,46} The three different

tube-guides/membranes of PVA (PVA, PVA-CNTs, and PVA-PPy) were physicochemical characterized prior to in vivo application. As a matter of fact, PVA with CNTs or PPy resulted in conductive biomaterials with higher electrical conductivity than the polymer matrix, and all the results were in agreement with the findings previously reported for such materials.^{13,24} The electrical conductivity achieved for the three different membranes (PVA, PVA-CNTs, and PVA-PPy) was 1.56×10^{-6} S/m, 579.6×10^{-6} S/m, and 1837.56×10^{-6} S/m, respectively (Table I), demonstrating that the electrical conductivity of PVA-PPy and PVA-CNTs are around 500 and 2000 times greater than the one observed to PVA alone, respectively.²⁴

It is crucial to combine both neuromuscular functional and morphological assessment, which was performed in the present described in vivo trials. It is not generally agreed which type of evaluation tool is the most useful descriptor of functional recovery; for this reason, the use of different methods for an overall assessment of nerve function has been recommended by several investigators⁴⁷ and it is applied in the present experimental work, including WRL and EPT functional tests, SFI, SSI, and kinematic analysis of the gait and morphometric analysis^{5,29} of the regenerated sciatic nerves and TA muscles. Among the wide range of available tests, EPT, SFI, SSI, and WRL, proved to be reliable, valid and efficient methods to determine

functional recovery after sciatic nerve injury in previous studies but with some subjectivity in the results analysis,^{5,30} so it is important to include the gait kinematic analysis and quantitative morpho-logical evaluation of the regenerated nerve and TA muscle.^{2,5} Indeed, the use of biomechanical parameters has given valuable insight into the effects of the sciatic nerve denervation/reinnervation, and thus represents an integration of the neural control acting on the ankle and foot muscles, which is very useful and accurate to evaluate different therapeutic approaches.^{25,37,47} It is important to realize that the number of kinematic variables (positions, velocities, and accelerations) required to describe one-step cycle is very high. Therefore, it is only through high speed digital cameras that we can achieve a full kinematic description during gait.⁴⁸ Significant improvement in motor deficit could be noticed from week-3 post-injury onwards and at week-12, a residual motor and nociceptive deficit were present in the three treated groups, with no statistical differences. Also, the SSI and SFI scores were not different between the three experimental groups, showing a more pronounced recovery at week-5 and week-2, respectively. At 12 weeks post-injury ankle kinematics improved in every group and at TO, normal ankle angle values were registered for all groups with the relative exception of the PVA group, demonstrating a better recovery to normal gait pattern in animals treated with PVA-CNTs and PVA-PPy. Anyway, one should bear in mind that individual joint kinematics either in control or nerve-injured animals is characterized by high variability, with notable differences between different animals and even from step to step.⁴⁹ Such high level of variability, which seems to be an intrinsic property of normal quadruped walking, might affect in some degree the precision of joint kinematic measures of functional recovery after nerve injury.²¹

The regenerated nerves and TA muscles were processed for morphology studies after the healing period of 12 weeks that included quantitative morphometry of myelinated nerve fibers and muscle fibers' cross section area and "minimal Feret's diameter" quantifications. Considering the morphometric evaluation of the TA muscle, in the PVA-PPy and PVA-CNTs treatment groups there were a 9% and 19% increase in terms of average fiber size area and a 5% and 10% increase in term of the "minimal Feret's diameter," respectively, when comparing to the untreated Control group.¹ It is also interesting to observe that not only the two most promising treatment groups (PVA-PPy and PVA-CNTs), but also the sham (Control) exhibited better scores than Pre crush (no lesion) group. These results should be explained by the increased nerve sprouting in the nerves submitted to the crush lesion which might have produced a significant effect in terms of promotion of the muscle' re-innervation. Similar results were also described in a previous work on tibial nerve crush injury, in which hyper-innervations of neuromuscular junctions (NMJs) were observed after injury and reverted back to the normal level at the same time as the functional recovery.⁵⁰ The recent published article by di Summa et al.,⁵¹ where collagen nerve tube-guides (Neuro-gen^{VR}) were used in vivo to promote peripheral nerve regeneration, combined with SCs, it was possible to demonstrate an improved distal stump sprouting. The sprouting was more pronounced in the experimental group where the SCs were derived from bone marrow mesenchymal stem cells (BM-MSCs) when compared to SCs derived from adipose tissue mesenchymal stem cells (AT-MSCs). Conversely, no significant differences were observed in proximal regeneration among all the experimental groups. BM-MSCs and AT-MSCs - loaded conduits showed a diffuse sprouting pattern, while loaded SCs showed an enhanced cone pattern and a typical sprouting along the conduits walls, suggesting an increased affinity for the collagen type I fibrillar structure. This observation is important and should be related to results obtained from the innervated muscle morphometry analysis. It should be kept in mind that the sprouting is also evaluated and a constant observation in the histomorphometry analysis of the regenerated peripheral nerve after axotomy and neurotmesis lesions, where different reconstruction strategies were tested in vivo in the rat sciatic nerve model by our research group for the past years.^{2,4,7-13,24,29,30} Mor-

phometrical analysis of the regenerated nerves showed no differences in terms of number of myelinated fibers and axon diameter between the three treated groups, but it is possible to appreciate statistically significant differences between PVA and PVA-CNTs groups in the evaluation of myelin thickness and g-ratio, and between PVA-PPY and PVA-CNTs as regards g-ratio evaluation. The PVA-CNTs group presented higher myelin thickness and lower g-ratio which proves a better maturation of myelinated fibers.

The histopathology of lung, liver, kidneys, and regional lymph nodes was performed to ensure the

biocompatibility of these biomaterials, mostly what concerns the possible concentration of CNTs in these organs after biodegradation. No alterations compatible with images of inflammation, degeneration, fibrosis or necrosis were detected and the negative results obtained with both Von Kossa and Masson-Fontana stains reinforced the absence of nanotubes and carbon deposits in all the analyzed organs. These results were in agreement with previous *in vitro* experiments using hMSCs from the umbilical cord matrix that proved the cytocompatibility of these three biomaterials.^{13,24} Also the biocompatibility of these biomaterials was already previously proven in the ovine model when it was used as a vascular prosthesis,⁴⁵ but also in the rat sciatic nerve neurotmesis injury model.¹³

In conclusion, the membranes of PVA-CNTs and PVA-PPy are biocompatible and have electrical conductivity, which was benefit to nerve regeneration in terms of neuromuscular morphological regeneration but also from functional recovery point of view. The higher electrical conductivity measured in PVA-CNTs membrane might be responsible for the best results obtained in terms of peripheral nerve regeneration, demonstrating higher myelin thickness and lower g-ratio which proves a better maturation of myelinated fibers and it is also in line with the trend observed in results of kinematics analysis. Also, the neurogenic atrophy of the TA muscle was less significant in the rats where the crushed sciatic nerve was enwrapped in PVA-CNTs membranes, as better results in terms of average fiber size area and “minimal Feret’s diameter” was observed. The results obtained sustain that PVA-CNTs membranes promote neuro-muscular regeneration, by improving functional recovery and myelination of the regenerated nerve fibers. In this way, the neurogenic atrophy of the TA muscle is not so pronounced due to the associated reduced healing period.

REFERENCES

1. Pereira T, Gartner A, Amorim I, Armada-da-Silva P, Gomes R, Pereira C, Franc¸a ML, Morais DM, Rodrigues MA, Lopes MA, and others. Biomaterials and Stem Cell Therapies for Injuries Associated to Skeletal Muscular Tissues. INTECH Open Access Publisher; 2013.
2. Pereira T, Gartner A, Amorim I, Almeida A, Caseiro AR, Armada-da-Silva PAS, Fregnan F, Varejao ASP, Santos JD, Bartolo PJ, and others. Promoting nerve regeneration in a neurotmesis rat model using poly(DL-lactide-epsilon-caprolactone) membranes and mesenchymal stem cells from the Wharton’s jelly: *In vitro* and *in vivo* analysis. *Biomed Res Int* 2014;2014:302659.
3. Kline DG. Spinal nerve root repair after brachial plexus injury. *J Neurosurg Spine* 2000;93:336–338.
4. Gartner A, Pereira T, Simoes MJ, Armada-da-Silva P, Franc¸a ML, Sousa R, Raimondo S, Shirotsaki Y, Nakamura Y, Hayakawa S, and others. Use of hybrid chitosan membranes and human mesenchymal stem cells from the Wharton jelly of umbilical cord for promoting nerve regeneration in an axonotmesis rat model. *Neural Regen Res* 2012;7:2247.
5. Gartner A, Pereira T, Gomes R, Luis AL, Franc¸a ML, Geuna S, Armada-da-Silva P, Mauricio AC. Mesenchymal Stem Cells from Extra-Embryonic Tissues for Tissue Engineering-Regeneration of the Peripheral Nerve. INTECH Open Access Publisher; 2013.
6. Pereira T, Armada-da-Silva PAS, Amorim I, Rema A, Caseiro AR, Gartner A, Rodrigues M, Lopes MA, Bartolo PJ, Santos JD and others. Effects of human mesenchymal stem cells isolated from Wharton’s jelly of the umbilical cord and conditioned media on skeletal muscle regeneration using a myectomy model. *Stem Cells Int* 2014;2014:376918.
7. Gartner A, Pereira T, Armada-da-Silva PAS, Amado S, Veloso AP, Amorim I, Ribeiro J, Santos JD, Barcia RN, Cruz P, and others. Effects of umbilical cord tissue mesenchymal stem cells (UCX(R)) on rat sciatic nerve regeneration after neurotmesis injuries. *J Stem Cells Regen Med* 2014;10:14–26.
8. Gartner A, Pereira T, Armada-da-Silva PAS, Amorim I, Gomes R, Ribeiro J, Franc¸a ML, Lopes C, Porto B, Sousa R, and others. Use of poly(DL-lactide-epsilon-caprolactone) membranes and mesenchymal stem cells from the Wharton’s jelly of the umbilical cord for promoting nerve regeneration in axonotmesis: *In vitro* and *in vivo* analysis. *Differentiation* 2012;84:355–365.
9. Ribeiro J, Gartner A, Pereira T, Gomes R, Lopes MA, Goncalves C, Varejao A, Luis AL, Mauricio AC.

Perspectives of employing mesenchymal stem cells from the Wharton's jelly of the umbilical cord for peripheral nerve repair. *Int Rev Neurobiol* 2013;108:79–120.

10. Luis AL, Rodrigues JM, Amado S, Veloso AP, Armada-Da-Silva PA, Raimondo S, Fregnan F, Ferreira AJ, Lopes MA, Santos JD, and others. PLGA 90/10 and caprolactone biodegradable nerve guides for the reconstruction of the rat sciatic nerve. *Microsurgery* 2007;27:125–137.
11. Luis AL, Rodrigues JM, Geuna S, Amado S, Shirosaki Y, Lee JM, Fregnan F, Lopes MA, Veloso AP, Ferreira AJ, and others. Use of PLGA 90:10 scaffolds enriched with in vitro-differentiated neural cells for repairing rat sciatic nerve defects. *Tissue Eng Part A* 2008;14:979–993.
12. Luis AL, Rodrigues JM, Lobato JV, Lopes MA, Amado S, Veloso AP, Armada-da-Silva PA, Raimondo S, Geuna S, Ferreira AJ and others. Evaluation of two biodegradable nerve guides for the reconstruction of the rat sciatic nerve. *Biomed Mater Eng* 2007;17:39–52.
13. Ribeiro J, Pereira T, Caseiro AR, Armada-da-Silva PAS, Pires I, Prada J, Amorim Amado S, Franc, a ML, Gonc, alves C, Lopes MA, and others. Evaluation of biodegradable electric conductive tube-guides and mesenchymal stem cells. *World J Stem Cells* 2015;7: 956.
14. George PM, Saigal R, Lawlor MW, Moore MJ, LaVan DA, Marini RP, Selig M, Makhni M, Burdick JA, Langer R, and others. Three-dimensional conductive constructs for nerve regeneration. *J Biomed Mater Res A* 2009;91:519–527.
15. Baker MI, Walsh SP, Schwartz Z, Boyan BD. A review of polyvinyl alcohol and its uses in cartilage and orthopedic applications. *J Biomed Mater Res B Appl Biomater* 2012;100:1451–1457.
16. Harun MH, Saion E, Kassim A, Mahmud E, Hussain MY, Mustafa IS. Dielectric properties of poly (vinyl alcohol)/polypyrrole com-posite polymer films. *J Adv Sci Arts* 2009;1:9–16.
17. Ghasemi-Mobarakeh L, Prabhakaran MP, Morshed M, Nasr-Esfahani MH, Baharvand H, Kiani S, Al-Deyab SS, Ramakrishna S. Application of conductive polymers, scaffolds and electrical stimulation for nerve tissue engineering. *J Tissue Eng Regen Med* 2011;5:e17–e35.
18. Martini F, Bartholomew E. *Essentials of Anatomy and Physiology*, 5th ed. New York: Benjamin Cummings; 2009.
19. Tria MA, Fusco M, Vantini G, Mariot R. Pharmacokinetics of nerve growth factor (NGF) following different routes of administration to adult rats. *Exp Neurol* 1994;127:178–183.
20. Pereira T, Ivanova G, Caseiro AR, Barbosa P, Bartolo PJ, Santos JD, Luis AL, Mauricio AC. MSCs conditioned media and umbilical cord blood plasma metabolomics and composition. *PLoS One* 2014;9:e113769.
21. Amado S, Rodrigues JM, Luis AL, Armada-da-Silva PA, Vieira M, Gartner A, Simoes MJ, Veloso AP, Fornaro M, Raimondo S, and others. Effects of collagen membranes enriched with in vitro-differentiated N1E-115 cells on rat sciatic nerve regeneration after end-to-end repair. *J Neuroeng Rehabil* 2010;7:7.
22. Amado S, Simoes MJ, Armada da Silva PA, Luis AL, Shirosaki Y, Lopes MA, Santos JD, Fregnan F, Gambarotta G, Raimondo S, and others. Use of hybrid chitosan membranes and N1E-115 cells for promoting nerve regeneration in an axonotmesis rat model. *Biomaterials* 2008;29:4409–4419.
23. Ribeiro J, Pereira T, Amorim I, Caseiro AR, Lopes MA, Lima J, Gartner A, Santos JD, Bartolo PJ, Rodrigues JM, and others. Cell therapy with human MSCs isolated from the umbilical cord Wharton jelly associated to a PVA membrane in the treatment of chronic skin wounds. *Int J Med Sci* 2014;11:979–987.
24. Gonc, alves C, Ribeiro J, Ribeiro J, Pereira T, Luis AL, Mauricio AC, Santos JD, Lopes MA. Preparation and characterization of electrical conductive PVA based materials for peripheral nerve guide tubes. *J Biomed Mater Res: Part A* 2016; 104: 1981–1987.
25. Varejao~ ASP CA, Meek MF, Bulas-Cruz J Melo-Pinto P, Raimondo S, Geuna S, Giacobini-Robecchi G. Functional and morphological assessment of a standardized rat sciatic nerve crush injury with a non-serrated clamp. *J Neurotrauma* 2004;21:1652–1670.
26. Luis A, Amado S, Geuna S, Rodrigues J, Simoes~ M, Santos J, Fregnan F, Raimondo S, Veloso AP, Ferreira A, and others. Long-

- term functional and morphological assessment of a standardized rat sciatic nerve crush injury with a non-serrated clamp. *J Neurosci Methods* 2007;163:92–104.
27. Beer GM, Steurer J, Meyer VE. Standardizing nerve crushes with a non-serrated clamp. *J Reconstr Microsurg* 2001;17:531–534.
 28. Masters DB, Berde CB, Dutta SK, Griggs CT, Hu D, Kupsky W, Langer R. Prolonged regional nerve blockade by controlled release of local anesthetic from a biodegradable polymer matrix. *Anesthesiology* 1993;79:340–346.
 29. Luis AL. Reparação de lesões do nervo periférico num modelo animal, in *Veterinary Clinics. Universidade do Porto*; 2008. Portugal, p 269.
 30. Mauricio AC, Gartner A, Armada-da-Silva P, Amado S, Pereira T, Veloso A, Varejão A, Luis A, Geuna S. Cellular Systems and Biomaterials for Nerve Regeneration in Neurotmesis Injuries. In: Pignatello R, editor. *Biomaterials Applications for Nanomedicine*. 2011. p 978–979.
 31. Shir Y, Zeltser R, Vatine JJ, Carmi G, Belfer I, Zangen A, Overstreet D, Raber P, Seltzer Z. Correlation of intact sensibility and neuropathic pain-related behaviors in eight inbred and out-bred rat strains and selection lines. *Pain* 2001;90:75–82.
 32. Varejão AS, Melo-Pinto P, Meek MF, Filipe VM, Bulas-Cruz J. Methods for the experimental functional assessment of rat sciatic nerve regeneration. *Neurol Res* 2004;26:186–194.
 33. Tralhammer JG, Vladimirova M, Bershinsky B, Strichartz G. Neurologic evaluation of the rat during sciatic nerve block with lidocaine. *Anesthesiology* 1995;82:1013–1025.
 34. Koka RHT. Quantification of functional recovery following rat sciatic nerve transection. *Exp Neurol* 2001;168:192–195.
 35. Bain JR, Mackinnon SE, Hunter DA. Functional evaluation of complete sciatic, peroneal, and posterior tibial nerve lesions in the rat. *Plast Reconstr Surg* 1989;83:129–138.
 36. Bervar M. Video analysis of standing - an alternative footprint analysis to assess functional loss following injury to the rat nerve sciatic. *J Neurosci Methods* 2000;102:109–116.
 37. Varejão AS, Cabrita AM, Meek MF, Bulas-Cruz J, Filipe VM, Gabriel RC, Ferreira AJ, Geuna S, Winter DA. Ankle kinematics to evaluate functional recovery in crushed rat sciatic nerve. *Muscle Nerve* 2003;27:706–714.
 38. Varejão ASP CA, Geuna S, Melo-Pinto P, Filipe VM, Gramsbergen A, Meek MF. Toe out angle: A functional index for the evaluation of sciatic nerve recovery in the rat model. *Exp Neurol* 2003;183: 695–699.
 39. Geuna S, Gigo-Benato D, Rodrigues Ade C. On sampling and sampling errors in histomorphometry of peripheral nerve fibers. *Microsurgery* 2004;24:72–76.
 40. Geuna S TP, Battistoni B, Guglielmone R. Verification of the two-dimensional disector, a method for the unbiased estimation of density and number of myelinated nerve fibers in peripheral nerves. *Ann Anat* 2000;182:23–34.
 41. Lacerda L, Ali-Boucetta H, Herrero MA, Pastorin G, Bianco A, Prato M, Kostarelos K. Tissue histology and physiology following intra-venous administration of different types of functionalized multi-walled carbon nanotubes. *Nanomedicine (Lond)* 2008;3:149–161.
 42. He C, Yang C, Li Y. Chemical synthesis of coral-like nanowires and nanowire networks of conducting polypyrrole. *Synth Met* 2003;139:539–545.
 43. Dellon AL, Mackinnon SE. Selection of the appropriate parameter to measure neural regeneration. *Ann Plast Surg* 1989;23:197–202.
 44. Varejão ASP CA, Meek MF, Fornaro M, Geuna S, Giacobini-Robecchi MG. Morphology of nerve fiber regeneration along a biodegradable poly (DLLA-E-CL) nerve guide filled with fresh skeletal muscle. *Microsurgery* 2003;23:338–345.
 45. Alexandre N, Ribeiro J, Gartner A, Pereira T, Amorim I, Fragoso J, Lopes A, Fernandes J, Costa E, Santos-Silva A, and others. Bio-compatibility and hemocompatibility of polyvinyl alcohol hydrogel used for vascular grafting-In vitro and in vivo studies. *J Biomed Mater Res A* 2014;102:4262–4275.
 46. Wood JA, Colletti E, Mead LE, Ingram D, Porada CD, Zanjani ED, Yoder MC, Almeida-Porada G.

- Distinct contribution of human cord blood-derived endothelial colony forming cells to liver and gut in a fetal sheep model. *Hepatology* 2012;56:1086–1096.
47. Morris J, Hudson A, Weddell G. A study of degeneration and regeneration in the divided rat sciatic nerve based on electron microscopy. IV. Changes in fascicular microtopography, perineurium and endoneurial fibroblasts. *Z Zellforsch Mikrosk Anat (Vienna, Austria: 1948)* 1971;124:165–203.
 48. Costa LM, Simoes MJ, Mauricio AC, Varejao AS. Methods and protocols in peripheral nerve regeneration experimental research: Part IV—kinematic gait analysis to quantify peripheral nerve regeneration in the rat. *Int Rev Neurobiol* 2009;87:127–139.
 49. Jacobson S, Guth L. An electrophysiological study of the early stages of peripheral nerve regeneration. *Exp Neurol* 1965;11:48–60.
 50. Ninagawa NT, Isobe E, Hirayama Y, Murakami R, Komatsu K, Nagai M, Kobayashi M, Kawabata Y, Torihashi S. Transplanted mesenchymal stem cells derived from embryonic stem cells promote muscle regeneration and accelerate functional recovery of injured skeletal muscle. *Biores Open Access* 2013;2:295–306.
 51. di Summa PG, Kingham PJ, Campisi CC, Raffoul W, Kalbermatten DF. Collagen (NeuraGen(R)) nerve conduits and stem cells for peripheral nerve gap repair. *Neurosci Lett* 2014;572:26–31.